Published in final edited form as:
Int J Biochem Cell Biol. 2009 June ; 41(6): 1371–1380. doi:10.1016/j.biocel.2008.12.002.

Enzymatically inactive adenylate kinase 4 interacts with mitochondrial ADP/ATP translocase

Rujuan Liu[1,2,3], **Anna-Lena Ström**[3], **Jianjun Zhai**[3], **Jozsef Gal**[3], **Shilai Bao**[4], **Weimin Gong**[1,2,*], and **Haining Zhu**[3,*]

1 *National Key Laboratory of Macrobiomolecules, Center for Structural and Molecular Biology, Institute of Biophysics, Chinese Academy of Sciences, Beijing, 100101, P. R. China*

2 *School of Life Sciences, University of Science and Technology of China, Hefei, Anhui, 230026, P. R. China*

3 *Department of Molecular and Cellular Biochemistry & Center for Structural Biology, College of Medicine, University of Kentucky, 741 South Limestone, Lexington, KY 40536-0509, USA*

4 *Institute of Genetics and Developmental Biology, Chinese Academy of Sciences, Beijing, 100101, P. R. China*

Abstract

Adenylate kinase 4 (AK4) is a unique member with no enzymatic activity *in vitro* in the adenylate kinase (AK) family although it shares high sequence homology with other AKs. It remains unclear what physiological function AK4 might play or why it is enzymatically inactive. In this study, we showed increased AK4 protein levels in cultured cells exposed to hypoxia and in an animal model of the neurodegenerative disease amyotrophic lateral sclerosis. We also showed that small hairpin RNA (shRNA)-mediated knockdown of AK4 in HEK293 cells with high levels of endogenous AK4 resulted in reduced cell proliferation and increased cell death. Furthermore, we found that AK4 over-expression in the neuronal cell line SH-SY5Y with low endogenous levels of AK4 protected cells from H_2O_2 induced cell death. Proteomic studies revealed that the mitochondrial ADP/ATP translocases (ANTs) interacted with AK4 and higher amount of ANT was co-precipitated with AK4 when cells were exposed to H_2O_2 treatment. In addition, structural analysis revealed that, while AK4 retains the capability of binding nucleotides, AK4 has a glutamine residue instead of a key arginine residue in the active site well conserved in other AKs. Mutation of the glutamine residue to arginine (Q159R) restored the adenylate kinase activity with GTP as substrate. Collectively, these results indicate that the enzymatically inactive AK4 is a stress responsive protein critical to cell survival and proliferation. It is likely that the interaction with the mitochondrial inner membrane protein ANT is important for AK4 to exert the protective benefits to cells under stress.

Keywords

adenylate kinase 4; mitochondrial ADP/ATP translocase; stress response; cell survival; enzymatic activity

* Address correspondence to: Haining Zhu (E-mail: haining@uky.edu, Tel 1-859-323-3643, Fax 1-859-257-2283) and Weimin Gong (E-mail: wgong@ibp.ac.cn, Tel 86-10-6488-8467, Fax 86-10-6488-8513).

Introduction

Adenylate kinases (AKs) are ubiquitous enzymes involved in energy metabolism and homeostasis of cellular adenine nucleotide composition (Noma, 2005). They catalyze the reversible transfer of a γ-phosphate group from Mg^{2+}ATP (or GTP) to AMP, releasing Mg^{2+}ADP (or GDP) and ADP (Khoo and Russell, 1972). AKs belong to the nucleoside monophosphate kinases (NMPKs) that include guanylate kinases, thymidylate kinases and UMP/CMP kinases. All NMPKs share a common α/β fold consisting of a β-sheet CORE surrounded by α-helices (Yan and Tsai, 1999). All AKs contain a central CORE domain with an ATP-binding P-loop, a LID domain, and an AMP-binding domain called AMP_{bind}. The CORE and AMP_{bind} domains are well conserved in all AKs, whereas the length of the LID domain is variable. The LID domain of the short form AKs is a single loop while the LID domain of the long form AKs forms a four-stranded anti-parallel β-sheet. In the absence of ligands, AKs form an "open" conformation in which the LID domain is distant from the CORE domain and AMP_{bind} regions (Diederichs and Schulz, 1991, Schlauderer and Schulz, 1996). Upon substrates or bi-substrate analog P1,P5-Di(Adenosine-5′)Pentaphosphate (Ap5A) binding, significant conformational changes occur to form a "closed" state in which both LID and AMP_{bind} domains move closer to the CORE to form the active site (Muller and Schulz, 1992, Berry et al., 1994, Abele and Schulz, 1995, Berry and Phillips, 1998, Bae and Phillips, 2004, Miron et al., 2004, Schlauderer et al., 1996, Muller and Schulz, 1993, Wild et al., 1997). More recent studies showed that substrate-free AK can also form the "close" conformation at the microsecond to millisecond time scale along the enzymatic reaction trajectory (Henzler-Wildman et al., 2007b, Henzler-Wildman et al., 2007a).

Six AK genes named AK1–AK6 have been identified in vertebrates. AK1, AK5 and AK6 are short forms while the long forms include AK2, AK3 and AK4. The AK enzymes are highly conserved in primary sequence except the recently characterized AK6 (Ren et al., 2005). Human AK4 was first reported based on its 58% homology to bovine AK3 (Xu et al., 1992), and was later found in the mammalian central nervous system (Yoneda et al., 1998). Both AK3 and AK4 are found in the mitochondrial matrix, but show different catalytic activities *in vitro*. Human AK3 exhibited high AK activity using GTP as a phosphate donor, whereas AK4 showed no AK activity *in vitro* (Noma et al., 2001). In contrast to the ubiquitous expression of AK3 in all tissues examined, the AK4 expression was shown to be tissue-specific: high levels in kidney, moderate levels in heart and liver, and low levels in brain (Noma et al., 2001). The crystal structure of human AK4 was available from Protein Data Bank (PDB: 2AR7 and 2BBW) and showed similar "open" and "closed" conformations. However, it is unclear how this highly conserved AK4 loses its AK activity.

The study of AKs have been focused on their enzymatic activities and structural characterization. However, the physiological function of the enzymatically inactive AK4 is largely unknown. Large scale genomic and proteomic studies in recent years identified AK4 gene expression changes under various stress conditions. The mRNA level of AK4 in mouse ATDC5 chondroprogenitor cells was up-regulated under hypoxia (Chen et al., 2006). Another cDNA array study revealed increased AK4 levels in response to oxidative stress in vascular smooth muscle cells (Vendrov et al., 2006). In addition, the AK4 protein levels in rat liver were affected by four hepatotoxicants, acetaminophen, amiodarone, tetracycline and carbon tetrachloride (Yamamoto et al., 2006). In this study, we showed increased AK4 protein levels in cultured cells exposed to hypoxia and in an animal model of amyotrophic lateral sclerosis (ALS), a neurodegenerative disease in which oxidative stress is implicated. We showed that shRNA knowdown of AK4 in HEK293 cells, which have high endogenous AK4 levels, resulted in reduced cell proliferation and increased cell death. AK4 over-expression in the neuronal cell line SH-SY5Y, which has low levels of endogenous AK4, protected cells from H_2O_2 induced cell death. We further identified mitochondrial ADP/ATP translocases (ANTs) as an

interacting partner of AK4 and showed that higher amount of ANT interacted with AK4 when cells were exposed to H_2O_2 treatment. Moreover, we identified a key residue in AK4 that is responsible for the loss of the AK activity. Collectively, the results indicate that the enzymatically inactive AK4 is a stress responsive protein and is likely to function through its interaction with the mitochondrial membrane protein ANT.

Materials and methods

Plasmids Construction

The coding region of human AK4 (hAK4) cDNA was generated by PCR using human brain cDNA library (Clontech). For bacterial expression in *E. coli*, the full-length hAK4 was fused with a hexahistidine tag at the C-terminus. *Nde* I and *Xho* I sites were introduced by PCR at the 5′ and 3′ ends of the coding sequence and were used to subclone the fragment into the pET22b bacterial expression vector (Novagen). The Q159R mutation of hAK4 was generated with the MutanBEST Kit (Takara) using the following primers: 5′ CGTTAGTCCAGCGGGAGGATG3′ and 5′GTTCACCAGTGACGTCATCAATAC3′. For eukaryotic expression of hAK4, the DNA fragment was subcloned with *Hind* III and *Bam* HI into the p3xFLAG-CMV14 mammalian expression vector (Sigma), and the plasmid was named as AK4-FLAG.

The coding region of human ANT cDNA was generated by PCR using human brain cDNA library (Clontech) as well. The fragment was subcloned into p3xFLAG-CMV14 with *Hind* III and *Bam* HI and named as ANT-FLAG. The 3xHA-tagged ANT plasmid (called ANT-HA) was constructed by subcloning the ANT encoding sequence into the *Hind* III and *Bam* HI sites of p3xHA-CMV14 (Gal et al., 2007).

Cell Culture and Transfection

Human embryonic kidney HEK293 cells were cultured at 37°C under 5% CO_2 and 95% air in Dulbecco's modified Eagle's medium (DMEM, Invitrogen) containing 5% fetal bovine serum (FBS, Invitrogen), 100 units/ml penicillin, and 100 μg/ml streptomycin. SH-SY5Y cells were cultured with DMEM containing 10% FBS. 80% confluent HEK293 cells were transfected with the indicated plasmids using Lipofectamine (Invitrogen) following the manufacturer's instruction. SH-SY5Y cells were transfected with corresponding plasmids using Fugene HD (Roche Applied Science) following the manufacturer's instruction.

Short Hairpin RNA (shRNA) Interference

The U6 promoter driven shRNA expression vector pDsU6 and the plasmid construction protocol have been previously reported by Bao et al (Bao et al., 2004). The target sites in the hAK4 coding region are AK4 shRNA1 (gtgatcacatggtctggaacc) and AK4 shRNA2 (gttctcccgcaagaagtggcc). All target sites were identified as unique sequences by BLAST analysis of the NCBI gene databank. The control plasmid was luciferase shRNA in the pDsU6 vector (Bao et al., 2004).

Cell Viability

Cell viability was assessed using the 3-(4, 5-dimethylthiazol-2-yl)-2, 5-diphenyl tetrazolium bromide (MTT) assay as described (Mosmann, 1983). The absorbance at 560 nm was measured using a 96-well microplate spectrophotometer (Power WaveTM XS, Biotek Instruments).

DAPI Staining

Cells were seeded to coverslip 24 hrs after shRNA transfection and cultured for 3 additional days. Cells were fixed with fresh 4% paraformaldehyde, washed with PBS for 3X, and stained

with 4′,6-diamidino-2-phenylindole (DAPI, H1200, Vector Laboratories) by adding 25 μl 1.5 μg/ml DAPI to each coverslip. The coverslip was sealed with nail polish and kept in dark for 2 hours at 4 °C. Fluorescence microscopy was performed using Nikon Eclipse 90i with a 40x objective. Ten random view fields with a total of approximately 300 cells were counted. Cells with condensed nuclei had smaller and brightly stained nuclei.

Clonogenic Assay

HEK293 cells were transfected with AK4 shRNA1, shRNA2 or control using Lipofectamine 2000 (Invitrogen). Twenty-four hr after transfection, cells were harvested and equal number of cells (3×10^3 cells) were replated at low density and cultured in DMEM media containing 10% FBS (Invitrogen) and 750 μg/ml G418 (Invitrogen) in 5% CO_2 and 95% air at 37 °C. The number of colonies formed over a 10-day period was counted in ten random view fields for each transfection. The experiment was repeated three times independently and the average number of colonies in three experiments was presented.

H_2O_2 and Hypoxia Treatment

DMEM medium containing 150 μM freshly prepared H_2O_2 (Sigma) was added to the SH-SY5Y cells for indicated periods of time. Cells were subsequently washed with warm (37°C) PBS for three times and cultured in regular DMEM without H_2O_2 for 6 hrs before the cell viability assay was performed. The control cells were subjected the same procedure except no H_2O_2 was used.

SH-SY5Y cells were split into 60 mm^2 plates and cultured under regular conditions overnight to attach to the dish. Cells were incubated in the hypoxia incubator with 5% CO_2 and 1% O_2 at 37°C for indicated period of time. For normoxic control, cells were incubated under 5% CO_2 and 95% air at 37°C for the same period of time.

Animals

Transgenic mouse strains over-expressing wild-type and G93A mutant SOD1 (Gurney et al., 1994) were maintained as hemizygotes at the University of Kentucky animal facility. Transgenic positives were identified using PCR as previously described (Zhang et al., 2007). G93A SOD1 transgenic mice were sacrificed at 125 days of age and age-matched wild-type SOD1 transgenic mice were used as controls. Mice were anesthetized with an intraperitoneal injection of 100 mg/kg ketamine and 10 mg/kg zylazine before they were transcardically perfused with 0.1 M PBS, pH 7.5. Spinal cords were dissected and stored at −80°C for further studies. All animal procedures were approved by the university IACUC committee.

FLAG Immunoprecipitation

HEK293 cells transfected with AK4-FLAG or ANT-FLAG were harvested and lysed in RIPA buffer (50mM Tris-HCl pH 7.4, 1% NP-40, 0.25% sodium deoxycholate, 150 mM NaCl, 1 mM EDTA) diluted from 10X RIPA buffer (Upstate, 20–188) supplemented with protease inhibitor mixture (Sigma, P8340, 1:1,000 dilution) and 1 mM PMSF. After pre-clearing at 10,000 × g for 10 min, the cell lysate was subjected to FLAG immunoprecipitation (IP) using the anti-FLAG M2 affinity gel (Sigma, A2220) for 3 hours at 4°C as previously described (Zhang et al., 2007). After washing 3 x with RIPA buffer, proteins were eluted with the FLAG peptide (Sigma) and subjected to SDS-PAGE analysis.

Mass Spectrometry Analysis and Protein Identification

The immunoprecipitated proteins were resolved by 12% SDS-PAGE and stained with Sypro Ruby fluorescence dye (Invitrogen/Molecular Probes). Protein bands were excised from the gel and subjected to in-gel trypsin digestion and LC-MS/MS analysis as previsouly described

(Fukada et al., 2004, Lu and Zhu, 2005). Briefly, both MS and MS/MS data were acquired by Qstar XL Q-TOF mass spectrometer (Applied Biosystems, Foster City, CA) under information-dependent acquisition mode. The LC-MS/MS data were subjected to database searches for protein identification using a local MASCOT search engine. Multiple databases (NCBInr, Swiss-Prot and MSDB) were searched using the parameters as previously described (Fukada et al., 2004, Lu and Zhu, 2005), yielding identification of proteins in each sliced gel band.

Cytochrome c release

SH-SY5Y cells were transfected with AK4-FLAG or FLAG control vector. Forty-eight hrs post transfection, cells were treated with 150 μM H_2O_2 for 1 hr, changed to normal medium for 2 hrs and harvested by centrifugation at 2,000 g for 10 min at 4°C. The control cells were subjected to the same procedure except no H_2O_2 was used. Subcellular fractionation was performed using the protocol described in (Shao et al., 2004). Briefly, cell pellets were washed with PBS and then suspended in a 5 volumes of buffer A (20 mM Hepes, 10 mM KCl, 1.5 mM $MgCl_2$, 1 mM EDTA, 1 mM EGTA, 1 mM DTT and 250mM sucrose) supplemented with proteases inhibitors (Roche Diagnostics). After incubating on ice for 20 min, the cells were lyzed by passing through 26-gauge needles 15 times. The cell lysates were subjected to sequential centrifugation at 1,000 × g and 12,000 × g, each for 10 min at 4°C, to pellet nuclei and heavy membranes. The supernatants were then centrifuged at 100,000 × g for 30 min at 4°C to pellet light membranes. The resulting supernatants were the cytosolic fractions and subjected to SDS-PAGE and Western blotting analysis using cytochrome c antibody (556432, BD-Pharmingen) and tubulin antibody (sc-8035, Santa Cruz Biotechnology).

Western Blotting Analysis

A rabbit polyclonal hAK4 antibody was raised in the Animal Center of the Institute of Genetics and Developmental Biology, Chinese Academy of Sciences using the purified recombinant hAK4 protein as the antigen. The anti-hAK4 antibody was purified by affinity column using purified recombinant hAK4. The specificity of the antibody was tested using recombinant hAK3 and hAK4 and the Western blotting showed that the antibody could specifically recognize hAK4 but not hAK3 (Supplementary Figure S1). In addition, only a single band at the same apparent molecular weight as the recombinant hAK4 was visualized in Western blot using this antibody in the study.

After SDS-PAGE, proteins were transferred onto nitrocellulose membranes in 25 mM Tris-HCl, 192 mM glycine, 20% (v/v) methanol. Membranes were blocked in 5% milk in TBS with 0.1% Tween-20 (TBST) at room temperature followed by incubation with the indicated primary antibodies in TBST. Anti-β-Actin (sc-1616, Santa Cruz Biotechnology) was used at 1:1,000 dilution and anti-hAK4 was used at 1:2,000 dilution; anti-ANT (MSA02, Mitoscience) and anti-VDAC (ab15895, Abcam) were used at 1:500 and 1:1000 dilution, respectively. After primary antibody incubation, membranes were washed 4 times with TBST and incubated with the indicated secondary antibodies in 5% milk in TBST at room temperature. Membranes were then washed with TBST before the protein of interest was visualized using Supersignal West Pico Enhanced Chemiluminescent (ECL) substrate (Pierce). Intensities of western blotting bands were quantified using the NIH Image J software.

Adenylate Kinase Enzymatic Activity Assay

The hAK4 and Q159R mutant hAK4 were expressed in *E. coli* BL21 (DE3) and purified using standard protocol as previously described (Hou et al., 2007). Briefly, protein expression was induced by 0.5 mM IPTG with overnight incubation at 16°C in LB. Cells were harvested by centrifugation and resuspended in 20 mM Tris-HCl (pH 7.5), 500 mM NaCl, 5 mM imidazole, 1 mM PMSF and sonicated. After insoluble material was removed by centrifugation, the protein was purified by affinity chromatography with a Chelating SepharoseTM Fast Flow (Amersham

Biosciences), followed by gel filtration chromatography with Superdex™ 75 (Amersham Biosciences).

The AK activities of purified hAK4 and Q159R mutant hAK4 were measured by a coupled pyruvate kinase(PK)/lactate dehydrogenase(LDH) assay. The 1.6 ml enzyme activity assay mixture contained 50 mM Tris-HCl buffer (pH=7.5), 0.2mM NADH, 2.0 mM P-enolpyruvate, 2.0 mM ATP or GTP, 2.0 mM AMP, 3.0 mM $MgCl_2$, 0.5mg/ml BSA, 120mM NaCl and 75mM KCl, 16 units PK and 32 units LDH. The reaction was started by addition of purified proteins. The reaction rate was measured by the decrease of absorbance at 340 nm with time.

Results

AK4 protein level increased in hypoxia-treated cells and spinal cords of ALS mice

Recent genomic and proteomic studies indicated that AK4 levels could change under various stress conditions (Chen et al., 2006, Vendrov et al., 2006, Yamamoto et al., 2006). For instance, the mRNA level of AK4 in mouse ATDC5 chondroprogenitor cells was up-regulated under hypoxia (Chen et al., 2006). We first tested the hAK4 levels in neuroblastoma SH-SY5Y cells under normoxic and hypoxic conditions and the results are shown in Figure 1A. The endogenous AK4 levels were rather low when the cells were cultured under regular conditions. Compared to freshly plated cells, the AK4 levels increased during the period of cell culture experiment. More importantly, after cells were cultured under hypoxic condition (5% CO_2 and 1% O_2) for 24 hours or longer, the AK4 levels were significantly higher than those in control cells cultured under normoxic conditions.

Oxidative stress has been implicated in neurodegenerative diseases including ALS (Wiedau-Pazos et al., 1996, Valentine et al., 2005, Bruijn et al., 2004), thus we next tested the AK4 levels in an animal model of ALS. Mutations in the gene encoding copper-zinc superoxide dismutase (SOD1) have been linked to a subset of familial ALS (Rosen et al., 1993, Deng et al., 1993). The transgenic mice expressing G93A mutant SOD1 is a commonly used ALS animal model (Gurney et al., 1994). In this study, we investigated the AK4 levels in the G93A mutant SOD1 transgenic mice and age-matched wild-type SOD1 transgenic mice. Since the motor neurons in spinal cord are preferentially impacted in the pathology in the transgenic mouse model, the spinal cords from three pairs of ALS and control mice were harvested, homogenized and subjected to AK4 Western blotting analysis. The representative results are shown in Figure 1B. The AK4 levels in the spinal cords of G93A transgenic mice were significantly higher than those in the wild-type SOD1 transgenic mice spinal cords. The results in Figure 1 support that the AK4 protein level increases in cultured cells and animals under oxidative stress.

AK4 was critical to cell survival

AK4 was reported to be highly expressed in kidney but low in the central nervous system (Noma et al., 2001). To investigate the functional significance of AK4, we used short hairpin RNA (shRNA) interference approach to knockdown the endogenous AK4 expression in human embryonic kidney (HEK293) cells. As shown in Figure 2A, the two shRNAs targeting different sequences of hAK4 effectively reduced endogenous AK4 protein expression compared to cells transfected with control shRNA. Compared to cells transfected with control shRNA, cells transfected with AK4 shRNA became clustered with morphology indicative of cell death (Figure 2B). DAPI staining experiment showed that the percentage of cells containing condensed nuclei increased from 10% to approximately 30% to 40% in cells transfected with AK4 shRNA (Figure 2C). MTT assay showed 60% to 80% cell death in cells transfected with AK4 shRNA (Figure 2D). A different cell viability using Trypan blue staining showed approximately 50% cell death in AK4 shRNA transfected cells (Supplementary Figure S2).

Moreover, the clone formation assay showed that cells transfected with AK4 shRNA formed only approximately 30% to 40% of the number of clones formed by control cells (Figure 2E). The results from the AK4 knockdown experiments suggest that AK4 is critical to cell survival and proliferation.

AK4 protected cells against H_2O_2 treatment

We next tested whether AK4 over-expression would protect cells from oxidative stress since chronic hypoxia has been demonstrated to cause oxidative stress (Clanton, 2007). SH-SY5Y cells were used in this experiment since their endogenous AK4 levels were low (Figure 3A). Transfection of AK4-FLAG resulted in over-expression of AK4 in SH-SY5Y cells (Figure 3A) and had no significant impact on cell viability without H_2O_2 treatment (Figure 3B, 0 hr). After cells transfected with the vector control were treated with 150 μM H_2O_2 for 45 min, 1 hr or 1.5 hrs, the percentage of viable cells decreased to approximately 60% to 40%. In contrast, the percentage of viable cells transfected with AK4-FLAG was approximately 95%, 70% and 60% after H_2O_2 treatment for 45 min, 1 hr or 1.5 hrs, respectively. The same experiment was carried out using Trypan blue staining as an alternative cell viability assay and similar results were obtained (Supplementary Figure S3). The above data suggest that AK4 over-expression can provide protective benefits to cells under H_2O_2 treatment.

AK4 interacted with the mitochondrial ADP/ATP translocase (ANT)

To understand how this enzymatically inactive AK4 functions, we performed IP and proteomics experiments to search for AK4 interacting proteins. HEK293 cells were transfected with AK4-FLAG or empty FLAG vector as control. Cells were harvested and lysed in RIPA buffer and the cell lysates were subjected to IP using anti-FLAG M2 affinity gel. The immunoprecipitated proteins were subjected to SDS-PAGE and the Sypro Ruby stained gel image is shown in Figure 4A. There were three bands (indicated by arrows) in the immunoprecipiation sample from the AK4-FLAG expressing cells that were clearly absent in the control sample. These three bands were excised from the gel, subjected to in-gel trypsin digestion and subsequent LC-MS/MS analysis. The proteins in the bands were identified as AK4, mitochondrial ADP/ATP translocase 2(ANT2), and mitochondrial heat shock protein 75 (MTHSP75).

ANT is a mitochondrial inner membrane protein that forms the mitochondrial intermembrane junctional complexes with mitochondrial outer membrane protein voltage-dependent anion channel (VDAC) (Crompton et al., 2002). An important function of the VDAC-ANT complex is to shuttle ADP into mitochondria and to pump ATP out of mitochondria, thus the proper function of the complex is critical to maintaining the cellular energy homeostasis (Dahout-Gonzalez et al., 2006). The identification of ANT as an AK4 interacting protein was consistent with the reported localization of ANT (mitochondrial inner membrane) and AK4 (mitochondrial matrix). To further confirm the interaction, the FLAG immunoprecipitated proteins were analyzed by Western blotting as shown in Figure 4B. The endogenous ANT was detected in the FLAG IP sample of cells transfected with AK4-FLAG, but not in the control sample. In addition, the mitochondrial outer membrane protein VDAC, which is known to interact with ANT, was also detected in the AK4-FLAG IP sample. Western blotting of ANT and VDAC showed similar expression levels between cells transfected with the AK4-FLAG plasmid or the FLAG control vector.

Reverse IP experiments were performed to further validate the interaction. ANT-FLAG or FLAG control vector was transfected into HEK293 cells and the cell lysates were subjected to FLAG IP as described above. As shown in Figure 4C, endogenous AK4 was detected in the ANT-FLAG IP sample, but not in the control sample. Moreover, VDAC was also co-precipitated with ANT-FLAG but not with FLAG vector control. Western blotting of the cell

lysates revealed similar AK4 and VDAC expression levels in cells transfected with ANT-FLAG or FLAG vector control. The co-precipitation experiments in both directions (Figure 4B and 4C) strongly support the interaction between AK4 and ANT, which was revealed by the proteomics analysis (Figure 4A).

Higher amount of AK4-interacting ANT and suppressed cytochrome c release in AK4 over-expressing cells under oxidative stress

It was shown earlier that AK4 over-expression could protect SH-SY5Y cells against H_2O_2 treatment (Figure 3). We next tested whether the AK4-ANT interaction changed when cells were treated with H_2O_2. Forty-eight hrs after SH-SY5Y cells were transfected with AK4-FLAG and ANT-HA, cells were exposed to 150 μM H_2O_2 for 1 hr, washed with warm PBS for 3 x, cultured in fresh DMEM for additional 3 hrs, and then harvested. The control cells were subjected to the same medium changes except no H_2O_2 was added in the treatment step. The cell lysates were subjected to FLAG IP and the co-precipitated proteins were analyzed by SDS-PAGE and Western blotting. As shown in Figure 5A, higher quantity of ANT was co-precipitated with AK4 in the SH-SY5Y cells treated with H_2O_2. In contrast, the amounts of precipitated AK4 were similar in both samples and the amounts of over-expressed AK4 and ANT also remained comparable in both cell lysates. These data suggest that more of the mitochondrial matrix protein AK4 would interact with the mitochondrial inner membrane protein ANT when cells are under H_2O_2 induced oxidative stress. This indicates that the interaction with ANT may be important for AK4 to provide its protective benefits to cells exposed to H_2O_2 treatment.

We further tested whether the increased AK4-ANT interaction had functional relevance. Since ANT and VDAC have been reported to form the mitochondrial permeability-transition pore (MPTP) and regulate the permeability of mitochondrial membrane (Crompton et al., 2002, Brenner and Grimm, 2006, Kroemer et al., 2007, Halestrap and Brennerb, 2003), we tested whether AK4 over-expression modulated cytochrome c release in H_2O_2 treated SH-SY5Y cells. The cytocrhome c levels in the cytosolic fraction of cells with AK4 or control transfection with or without 1 hr 150 μM H_2O_2 treatment were assessed by Western blotting. A representative Western blot image and the quantitative results from three independent experiments are shown in Figure 5B. Compared to cells without H_2O_2 treatment, higher levels of cytochrome c were observed in both AK4 over-expressing and control cells after 1 hr H_2O_2 treatment ($p < 0.01$). More importantly, significantly less cytochrome c release was observed in the cytosolic fraction of the AK4 over-expressing cells, in comparison to the cells transfected with FLAG control vector (Lane 4 versus Lane 3, $p = 0.01$). The results suggest that AK4 over-expression can suppress, but not completely block, cytochrome c release from mitochondria to cytosol in SH-SY5Y cells under oxidative stress. The data supports that AK4 may modulate ANT function through its interaction with ANT to provide its protective benefits to cells exposed to H_2O_2.

Structural basis for the retained nucleotide binding capability and the lost adenylate kinase activity of AK4

Since AK4 is enzymatically inactive *in vitro*, its physiological function may not require the kinase activity. The results in this study suggest that it may function through interaction with ANT, a protein that is critical to ADP/ATP homeostasis in mitochondria. Thus, we hypothesize that AK4 likely retains the capability of binding nucleotides. Structures of substrate-free AK4 and diguanosine pentaphosphate (GP5)-bound AK4 (PDB entries 2AR7 and 2BBW) have been determined and showed highly conserved structures similar to other AKs (Diederichs and Schulz, 1991, Muller and Schulz, 1992, Berry et al., 1994, Abele and Schulz, 1995). AK4 also adopts “open” and “close” conformations in the absence and presence of substrate analog, respectively. Structural based sequence alignment was performed using Espript (Figure 6A).

Both the AMP binding motif and the P-loop responsible for NTP binding (indicated in Figure 6A) are well conserved, supporting that AK4 likely retains the nucleotide binding capability.

We further compared the active site of AK4 to the site in other enzymatically active AKs to determine the structural basis of the inactivity of AK4. The structural superposition of the active sites of human AK4 and *E. coli* AK is shown in Figure 6B. The active site residues are also well conserved in all of the AKs except that a key arginine residue conserved among other AKs is glutamine in AK4 from multiple organisms (Gln159 in human AK4). This conserved arginine residue has been reported to be critical to the AK activity (Yan et al., 1990). In the enzymatically active AKs, the phosphoryl group transfer involves a penta-coordinated transition state with the leaving γ-phosphoryl group of NTP and the nucleophilic α-phosphoryl group of AMP in two apical positions (Knowles, 1980). The transferred phosphoryl group is stabilized by the conserved arginine and another lysine residues nearby. In the crystal structure of *E. coli* AK bound with Ap5A (Muller and Schulz, 1992), the transferred phosphoryl group is stabilized by Lys13, Arg123, Arg156 and Arg167 (*E. coli* AK numbering). Lys13, Arg123 and Arg167 are conserved in all AKs including AK4 (indicated by * in Figure 6A). However, in the position of Arg156 in *E. coli* AK, a glutamine residue (Gln159, human AK4 numbering) is in human AK4 (indicated by a triangle in Figure 6A). The guanidinium group of Arg156 in *E.coli* AK form hydrogen bonds to both the nucleophilic and the leaving phosphoryl groups. However, the corresponding residue Gln159 in human AK4 is far away from the transferred phosphoryl group of GP5 (Figure 6B), thus unable to stabilize the reaction intermediate. Based on the above analysis, we hypothesized that this Gln159 in AK4 might compromise its ability of phosphoryl group transfer.

To test this hypothesis regarding the role of Gln159 in AK4 activity, mutant Q159R AK4 was expressed and purified. AK activity was measured using GTP or ATP as the phosphoryl donor. The native AK4 did not show any activity as reported. However, the Q159R mutant significantly restored the AK activity when GTP was used as the phosphoryl donor. This is similar to human AK3 that also needs GTP as substrate for its kinase activity (Noma et al., 2001). The specific activity of the Q159R AK4 mutant was 842 nmol/min/mg protein (Figure 6C). The above data strongly suggest that AK4 is a nucleotide binding protein but has lost the ability of catalyzing the phosphoryl group transfer reaction. The results also elucidated the structural basis for such characteristics of AK4.

Discussion

AK4 is a unique member of the adenylate kinases (AK) family since it shows no enzymatic activity *in vitro* although it shares high sequence homology with other AKs. This is in direct contrast to AK3 that is also localized in the mitochondrial matrix as AK4. The physiological function of AK4 is largely unknown, however recent large-scale genomic studies suggested that it could respond to various stress conditions (Chen et al., 2006, Vendrov et al., 2006, Yamamoto et al., 2006). In this study, we strive to establish the functional importance of AK4. We first examined the AK4 protein level in SH-SY5Y cells exposed to hypoxia using an AK4 polyclonal antibody we generated. The endogenous AK4 level in SH-SY5Y cells was low, consistent with the previous report of low AK4 expression in brain (Noma et al., 2001). When cells were exposed to hypoxia, the AK4 protein level increased significantly within 24 hrs and kept increasing up to the end-point of the experiment (72 hrs) (Figure 1A). Moreover, we tested the AK4 levels in a commonly used transgenic mouse model of ALS, a neurodegenerative disease in which oxidative stress has been implicated. As shown in Figure 1B, the AK4 level was significantly higher in the spinal cords of the transgenic mice expressing the ALS-causing SOD1 mutant G93A, compared to the transgenic mice expressing wild-type SOD1. The results clearly support that the endogenous level of AK4 protein increase in response to various stress

in cultured cells as well as in an animal model of human disease, suggesting that AK4 might provide protective benefits to cells under stress.

We next modulated the AK4 level by shRNA or over-expression to determine the effect of AK4 on cell survival. When AK4 expression was suppressed by shRNA in HEK293 cells with high endogenous AK4 levels, cell death increased and cell proliferation measured by clone formation decreased (Figure 2). When AK4 was over-expressed in SH-SY5Y cells with low endogenous AK4 levels, cell survival increased after H_2O_2 treatment compared to cells without AK4 over-expression (Figure 3). The results support the hypothesis that AK4 can be protective to cells under H_2O_2 induced oxidative stress.

To investigate the mechanism of how this enzymatically inactive protein functions *in vivo*, we used a proteomic approach to identify AK4 interacting partners. As shown in Figure 4, we identified three unique proteins that were not in the control IP sample: MTHSP75, AK4 and ADP/ATP translocase (ANT). MTHSP75 is a mitochondrial molecular chaperone that has been found to interact with multiple proteins (Bhattacharyya et al., 1995). More interestingly, ANT is a mitochondrial inner membrane protein that forms a complex with the mitochondrial outer membrane protein voltage dependent anion channel (VDAC). The interaction of AK4 with the ANT/VDAC complex was further validated by bi-directional co-immonoprecipitation experiments (Figure 4B and 4C). To our knowledge, the results are the first reporting the interaction between AK4 and the ANT/VDAC complex.

ATP is produced in the mitochondrial matrix through the oxidative phosphorylation process by ATP synthase, and the release of ATP into the cytosol as well as the ADP exchanged into mitochondrial matrix is performed by ANT (Dahout-Gonzalez et al., 2006). Since the homeostasis of ADP/ATP is critical to cell survival and proliferation, it is logical to propose that AK4 can interact with the ANT/VDAC complex, modulate the ADP/ATP homeostasis, and consequently influence cell survival and proliferation. Alternatively, ANT and VDAC are reported to form the mitochondrial permeability-transition pore (MPTP), which can regulate the permeability of mitochondrial membrane and subsequently the cell death pathway (Crompton et al., 2002, Brenner and Grimm, 2006, Kroemer et al., 2007, Halestrap and Brennerb, 2003). We hypothesize that AK4 may modulate the mitochondrial membrane permeability via its interaction with ANT. Consistent with this hypothesis, we observed that the amount of ANT co-precipitated with AK4 increased in cells treated with H_2O_2 (Figure 5), i.e. the affinity and/or dynamics of the interaction between AK4 and ANT changed when cells responded to stresses. We further tested cytochrome c release from mitochondria to cytosol in SH-SY5Y cells exposed to H_2O_2 and found that cytochrome c release was suppressed in AK4 over-expressing cells. These results support the hypothesis that AK4 may function through the interaction with ANT. Future studies need to be carried out to determine how AK4 modulates the properties of the ANT/VDAC complex. For instance, how would ADP/ATP homeostasis or mitochondrial membrane permeability be influenced by AK4? Nevertheless, the interaction with the ANT/VDAC complex appears to be critical to the physiological function of AK4 as a stress responsive protein.

The notion that AK4 functions through interacting with ANT is also supported by other evidence. First, AK4 has been reported to be localized in the mitochondrial matrix, thus the interaction between AK4 and the mitochondrial inner membrane protein ANT is likely to occur under physiological conditions. Second, the structure-based sequence alignment has revealed complete reservation of the residues responsible for nucleotide binding (Figure 6A). Thus AK4 is able to bind NDP and NTP, providing functional relevance to interact with ANT, the protein responsible for homeostasis of ADP and ATP. Third, the structural superposition of AK4 with other AKs with kinase activity revealed that a key arginine residue involved in the phosphoryl group transfer is replaced with a glutamine residue in AK4 (Figure 6B). Mutagenesis of the

glutamine to arginine (Q159R) restored the kinase activity using GTP as substrate (Figure 6C). The results in this study clearly illustrate the structural basis of the inactive enzyme. In addition, the results also support that AK4 is more likely to play a regulatory role by interacting with ANT rather than catalyzing the adenylate kinase reaction. In fact, a recent study showed that another AK family member AK2 could activate a novel cell apoptotic pathway through formation of a complex with FADD and caspase-10, which was independent of its adenylate kinase activity (Lee et al., 2007).

In conclusion, this study provides new insights into the function and significance of AK4, an enzymatically inactive AK whose function had been largely unknown. The results demonstrate that AK4 provides protective benefits to cells under various stresses and that AK4 interacts with the ANT/VDAC complex. It is also suggested that AK4 likely accomplishes its function by interacting with and modulating the ANT/VDAC complex. It remains to be determined in future studies how AK4 interacts with the ANT/VDAC complex and modulates its properties under physiological and pathological conditions.

Supplementary Material

Refer to Web version on PubMed Central for supplementary material.

Acknowledgements

This work is partially supported by NIH/NINDS R01 grant (R01NS049126), NIH/NCRR COBRE grant (P20RR020171) and NIH/NIEHS Superfund Basic Research Program grant (P42ES 07380) to H.Z. W.G. has been supported by Chinese National Funding for Talent Youth (Grant No. 30225015), Ministry of Science and Technology (Grant Nos. 2004CB720008, 2006CB0D1705, 2007CB914304), 863 program (2006AA02A316), the National Natural Science Foundation of China (Grant No 10490193) and the Chinese Academy of Sciences (KSCX2-YW-R-61). The Overseas Young Investigator Award to H.Z. and W. G. from the National Natural Science Foundation of China (Grant No 30728004) is acknowledged. We thank Dr. Natasha Kyprianou for allowing us to use the hypoxia incubator.

Abbreviations

AK
: adenylate kinase

AK4
: adenylate kinase 4

NMPK
: nucleoside monophosphate kinase

ANT
: mitochondrial ADP/ATP translocase

VDAC
: voltage dependent anion channel

MPTP
: mitochondrial permeability transition pore

shRNA
: short hairpin RNA

DAPI
: 4′,6-diamidino-2-phenylindole

IP

immunoprecipitation

MS

mass spectrometry

LC-MS

liquid chrotamography-mass spectrometry

ALS

amyotrophic lateral sclerosis

SOD1

cooper-zinc superoxide dismutase

Ap5A

P1,P5-Di(Adenosine-5′)Pentaphosphate

References

Abele U, Schulz GE. High-resolution structures of adenylate kinase from yeast ligated with inhibitor Ap5A, showing the pathway of phosphoryl transfer. Protein Sci 1995;4:1262–1271. [PubMed: 7670369]

Bae E, Phillips GN Jr. Structures and analysis of highly homologous psychrophilic, mesophilic, and thermophilic adenylate kinases. J Biol Chem 2004;279:28202–28208. [PubMed: 15100224]

Bao S, Lu T, Wang X, Zheng H, Wang LE, Wei Q, Hittelman WN, Li L. Disruption of the Rad9/Rad1/Hus1 (9-1-1) complex leads to checkpoint signaling and replication defects. Oncogene 2004;23:5586–5593. [PubMed: 15184880]

Berry MB, Meador B, Bilderback T, Liang P, Glaser M, Phillips GN Jr. The closed conformation of a highly flexible protein: the structure of E. coli adenylate kinase with bound AMP and AMPPNP. Proteins 1994;19:183–198. [PubMed: 7937733]

Berry MB, Phillips GN Jr. Crystal structures of Bacillus stearothermophilus adenylate kinase with bound Ap5A, Mg2+ Ap5A, and Mn2+ Ap5A reveal an intermediate lid position and six coordinate octahedral geometry for bound Mg2+ and Mn2+ Proteins 1998;32:276–288. [PubMed: 9715904]

Bhattacharyya T, Karnezis AN, Murphy SP, Hoang T, Freeman BC, Phillips B, Morimoto RI. Cloning and subcellular localization of human mitochondrial hsp70. J Biol Chem 1995;270:1705–1710. [PubMed: 7829505]

Brenner C, Grimm S. The permeability transition pore complex in cancer cell death. Oncogene 2006;25:4744–4756. [PubMed: 16892087]

Bruijn LI, Miller TM, Cleveland DW. Unraveling the mechanisms involved in motor neuron degeneration in ALS. Annu Rev Neurosci 2004;27:723–749. [PubMed: 15217349]

Chen L, Fink T, Ebbesen P, Zachar V. Temporal transcriptome of mouse ATDC5 chondroprogenitors differentiating under hypoxic conditions. Exp Cell Res 2006;312:1727–1744. [PubMed: 16580664]

Clanton TL. Hypoxia-induced reactive oxygen species formation in skeletal muscle. J Appl Physiol 2007;102:2379–2388. [PubMed: 17289907]

Crompton M, Barksby E, Johnson N, Capano M. Mitochondrial intermembrane junctional complexes and their involvement in cell death. Biochimie 2002;84:143–152. [PubMed: 12022945]

Dahout-Gonzalez C, Nury H, Trezeguet V, Lauquin GJ, Pebay-Peyroula E, Brandolin G. Molecular, functional, and pathological aspects of the mitochondrial ADP/ATP carrier. Physiology (Bethesda) 2006;21:242–249. [PubMed: 16868313]

Deng HX, Hentati A, Tainer JA, Iqbal Z, Cayabyab A, Hung WY, Getzoff ED, Hu P, Herzfeldt B, Roos RP, et al. Amyotrophic lateral sclerosis and structural defects in Cu, Zn superoxide dismutase. Science 1993;261:1047–1051. [PubMed: 8351519]

Diederichs K, Schulz GE. The refined structure of the complex between adenylate kinase from beef heart mitochondrial matrix and its substrate AMP at 1.85 A resolution. J Mol Biol 1991;217:541–549. [PubMed: 1994037]

Fukada K, Zhang F, Vien A, Cashman NR, Zhu H. Mitochondrial proteomic analysis of a cell line model of familial amyotrophic lateral sclerosis. Mol Cell Proteomics 2004;3:1211–1223. [PubMed: 15501831]

Gal J, Strom AL, Kilty R, Zhang F, Zhu H. p62 accumulates and enhances aggregate formation in model systems of familial amyotrophic lateral sclerosis. J Biol Chem 2007;282:11068–11077. [PubMed: 17296612]

Gurney ME, Pu H, Chiu AY, Dal Canto MC, Polchow CY, Alexander DD, Caliendo J, Hentati A, Kwon YW, Deng HX, et al. Motor neuron degeneration in mice that express a human Cu, Zn superoxide dismutase mutation. Science 1994;264:1772–1775. [PubMed: 8209258]

Halestrap AP, Brennerb C. The adenine nucleotide translocase: a central component of the mitochondrial permeability transition pore and key player in cell death. Curr Med Chem 2003;10:1507–1525. [PubMed: 12871123]

Henzler-Wildman KA, Lei M, Thai V, Kerns SJ, Karplus M, Kern D. A hierarchy of timescales in protein dynamics is linked to enzyme catalysis. Nature 2007a;450:913–916. [PubMed: 18026087]

Henzler-Wildman KA, Thai V, Lei M, Ott M, Wolf-Watz M, Fenn T, Pozharski E, Wilson MA, Petsko GA, Karplus M, Hubner CG, Kern D. Intrinsic motions along an enzymatic reaction trajectory. Nature 2007b;450:838–844. [PubMed: 18026086]

Hou X, Liu R, Ross S, Smart EJ, Zhu H, Gong W. Crystallographic studies of human MitoNEET. J Biol Chem 2007;282:33242–33246. [PubMed: 17905743]

Khoo JC, Russell PJ. Isoenzymes of adenylate kinase in human tissue. Biochim Biophys Acta 1972;268:98–101. [PubMed: 5018282]

Knowles JR. Enzyme-catalyzed phosphoryl transfer reactions. Annu Rev Biochem 1980;49:877–919. [PubMed: 6250450]

Kroemer G, Galluzzi L, Brenner C. Mitochondrial membrane permeabilization in cell death. Physiol Rev 2007;87:99–163. [PubMed: 17237344]

Lee HJ, Pyo JO, Oh Y, Kim HJ, Hong SH, Jeon YJ, Kim H, Cho DH, Woo HN, Song S, Nam JH, Kim HJ, Kim KS, Jung YK. AK2 activates a novel apoptotic pathway through formation of a complex with FADD and caspase-10. Nat Cell Biol 2007;9:1303–1310. [PubMed: 17952061]

Lu X, Zhu H. Tube-gel digestion: a novel proteomic approach for high throughput analysis of membrane proteins. Mol Cell Proteomics 2005;4:1948–1958. [PubMed: 16150870]

Miron S, Munier-Lehmann H, Craescu CT. Structural and dynamic studies on ligand-free adenylate kinase from Mycobacterium tuberculosis revealed a closed conformation that can be related to the reduced catalytic activity. Biochemistry 2004;43:67–77. [PubMed: 14705932]

Mosmann T. Rapid colorimetric assay for cellular growth and survival: application to proliferation and cytotoxicity assays. J Immunol Methods 1983;65:55–63. [PubMed: 6606682]

Muller CW, Schulz GE. Structure of the complex between adenylate kinase from Escherichia coli and the inhibitor Ap5A refined at 1.9 A resolution. A model for a catalytic transition state. J Mol Biol 1992;224:159–177. [PubMed: 1548697]

Muller CW, Schulz GE. Crystal structures of two mutants of adenylate kinase from Escherichia coli that modify the Gly-loop. Proteins 1993;15:42–49. [PubMed: 8451239]

Noma T. Dynamics of nucleotide metabolism as a supporter of life phenomena. J Med Invest 2005;52:127–136. [PubMed: 16167529]

Noma T, Fujisawa K, Yamashiro Y, Shinohara M, Nakazawa A, Gondo T, Ishihara T, Yoshinobu K. Structure and expression of human mitochondrial adenylate kinase targeted to the mitochondrial matrix. Biochem J 2001;358:225–232. [PubMed: 11485571]

Ren H, Wang L, Bennett M, Liang Y, Zheng X, Lu F, Li L, Nan J, Luo M, Eriksson S, Zhang C, Su XD. The crystal structure of human adenylate kinase 6: An adenylate kinase localized to the cell nucleus. Proc Natl Acad Sci U S A 2005;102:303–308. [PubMed: 15630091]

Rosen DR, Siddique T, Patterson D, Figlewicz DA, Sapp P, Hentati A, Donaldson D, Goto J, O'Regan JP, Deng HX, et al. Mutations in Cu/Zn superoxide dismutase gene are associated with familial amyotrophic lateral sclerosis. Nature 1993;362:59–62. [PubMed: 8446170]

Schlauderer GJ, Proba K, Schulz GE. Structure of a mutant adenylate kinase ligated with an ATP-analogue showing domain closure over ATP. J Mol Biol 1996;256:223–227. [PubMed: 8594191]

Schlauderer GJ, Schulz GE. The structure of bovine mitochondrial adenylate kinase: comparison with isoenzymes in other compartments. Protein Sci 1996;5:434–441. [PubMed: 8868479]

Shao Y, Gao Z, Marks PA, Jiang X. Apoptotic and autophagic cell death induced by histone deacetylase inhibitors. Proc Natl Acad Sci U S A 2004;101:18030–18035. [PubMed: 15596714]

Valentine JS, Doucette PA, Zittin Potter S. Copper-zinc superoxide dismutase and amyotrophic lateral sclerosis. Annu Rev Biochem 2005;74:563–593. [PubMed: 15952898]

Vendrov AE, Madamanchi NR, Hakim ZS, Rojas M, Runge MS. Thrombin and NAD(P)H Oxidase-Mediated Regulation of CD44 and BMP4-Id Pathway in VSMC, Restenosis, and Atherosclerosis. Circ Res 2006;98:1254–1263. [PubMed: 16601225]

Wiedau-Pazos M, Goto JJ, Rabizadeh S, Gralla EB, Roe JA, Lee MK, Valentine JS, Bredesen DE. Altered reactivity of superoxide dismutase in familial amyotrophic lateral sclerosis. Science 1996;271:515–518. [PubMed: 8560268]

Wild K, Grafmuller R, Wagner E, Schulz GE. Structure, catalysis and supramolecular assembly of adenylate kinase from maize. Eur J Biochem 1997;250:326–331. [PubMed: 9428681]

Xu G, O'Connell P, Stevens J, White R. Characterization of human adenylate kinase 3 (AK3) cDNA and mapping of the AK3 pseudogene to an intron of the NF1 gene. Genomics 1992;13:537–542. [PubMed: 1639383]

Yamamoto T, Kikkawa R, Yamada H, Horii I. Investigation of proteomic biomarkers in in vivo hepatotoxicity study of rat liver: toxicity differentiation in hepatotoxicants. J Toxicol Sci 2006;31:49–60. [PubMed: 16538043]

Yan H, Tsai MD. Nucleoside monophosphate kinases: structure, mechanism, and substrate specificity. Adv Enzymol Relat Areas Mol Biol 1999;73:103–134. x. [PubMed: 10218107]

Yan HG, Shi ZT, Tsai MD. Mechanism of adenylate kinase. Structural and functional demonstration of arginine-138 as a key catalytic residue that cannot be replaced by lysine. Biochemistry 1990;29:6385–6392. [PubMed: 2119801]

Yoneda T, Sato M, Maeda M, Takagi H. Identification of a novel adenylate kinase system in the brain: cloning of the fourth adenylate kinase. Brain Res Mol Brain Res 1998;62:187–195. [PubMed: 9813319]

Zhang F, Strom AL, Fukada K, Lee S, Hayward LJ, Zhu H. Interaction between familial amyotrophic lateral sclerosis (ALS)-linked SOD1 mutants and the dynein complex. J Biol Chem 2007;282:16691–16699. [PubMed: 17403682]

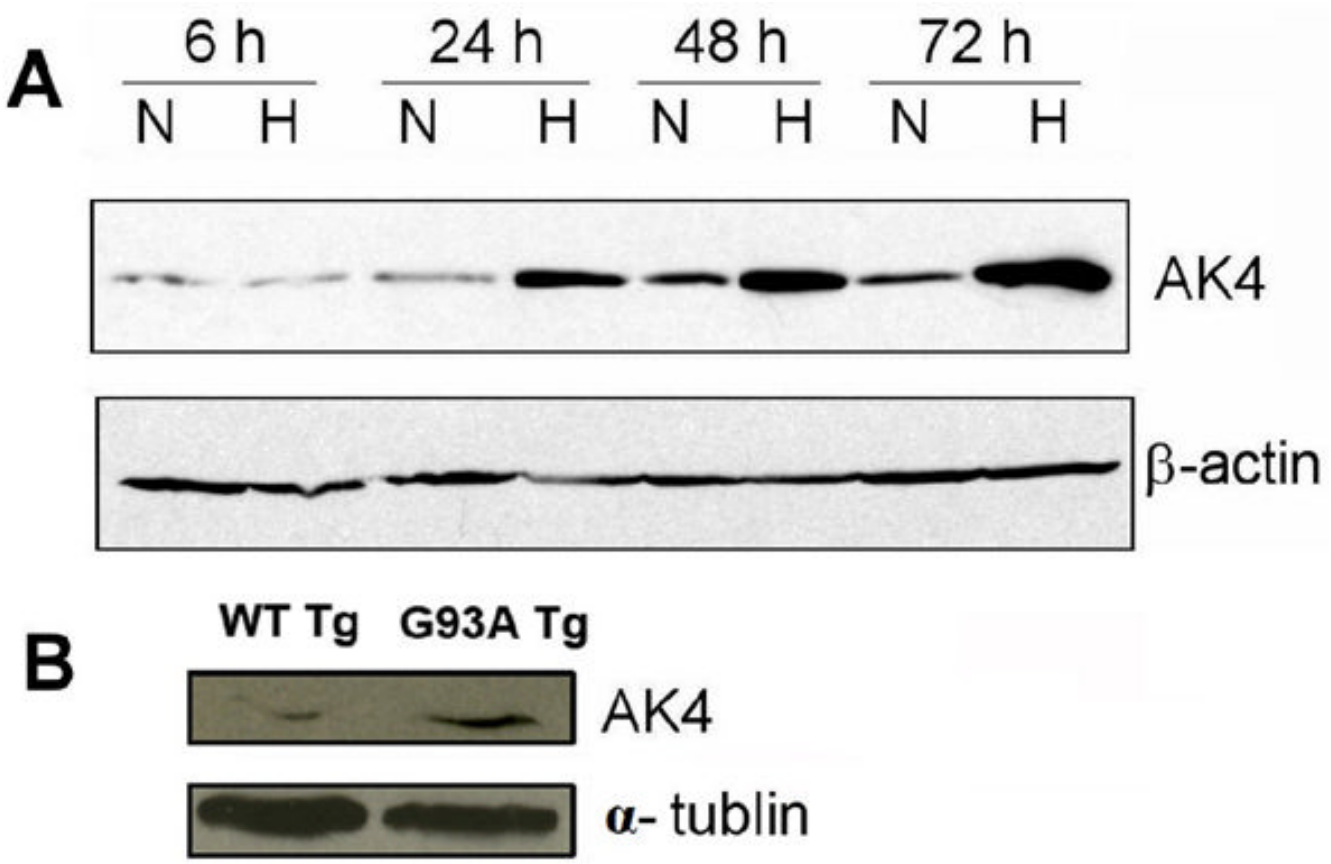

Figure 1. AK4 protein expression level change under stress and in disease

(A). AK4 protein levels in SH-SY5Y cells under normal or hypoxia conditions. "N" = normal; "H" = hypoxia. **(B).** AK4 protein levels in the spinal cords of wild-type SOD1 and G93A mutant SOD1 transgenic mice.

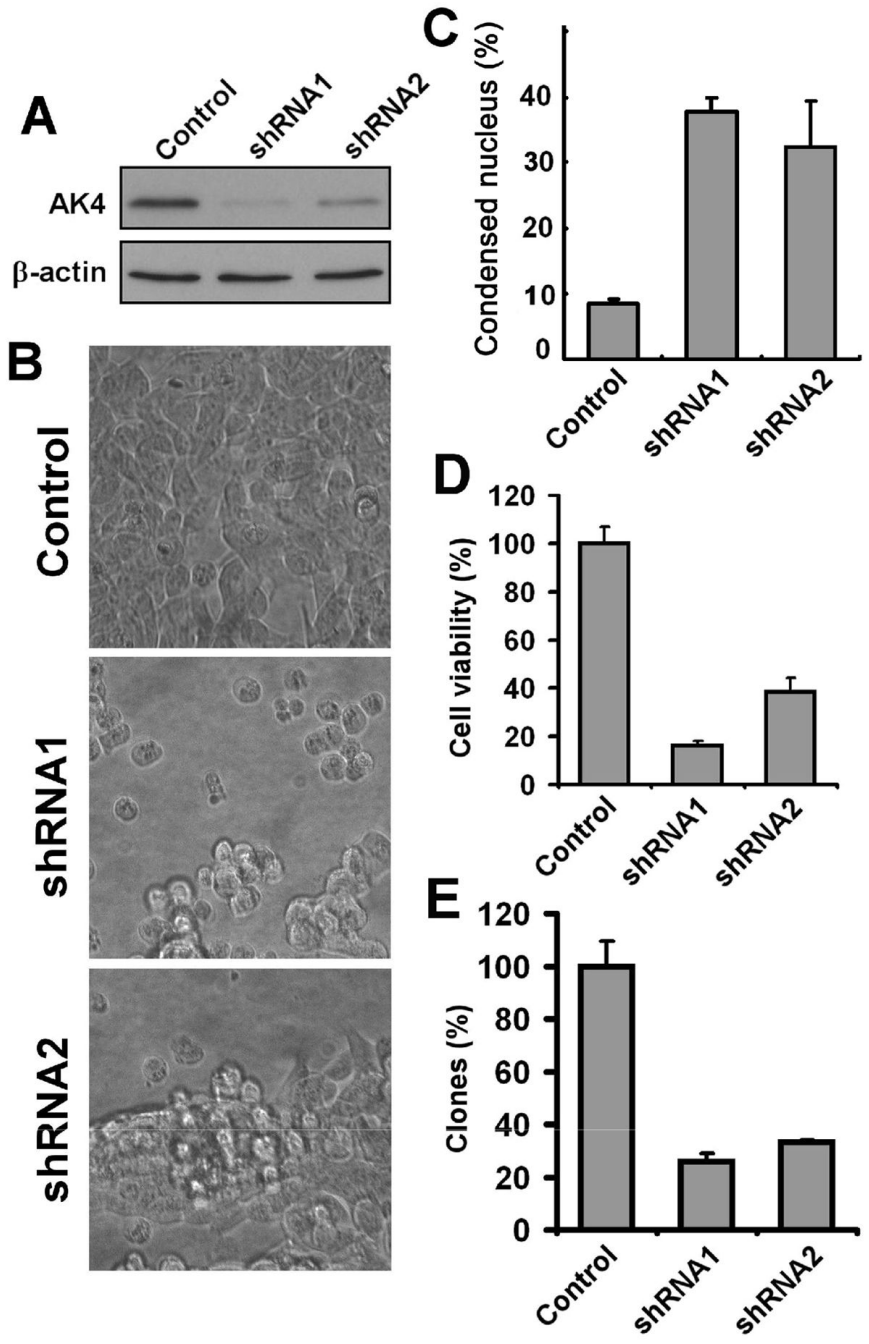

Figure 2. AK4 shRNA silencing suppressed HEK293 cell survival and proliferation

(A). Western blotting of AK4 in HEK293 cells transfected with human AK4 shRNAs targeting two different regions of AK4 coding sequence.**(B).** Representative images of HEK293 cells transfected with AK4 shRNA or control. **(C).** The percentage of cells with condensed nuclei 4 days after AK4 shRNA silencing. Cells were stained by DAPI and 10 random view fields with approximately 300 cells were counted for each sample. **(D).** The percentage of viable HEK293 cells 6 days after AK4 shRNA silencing. The viability was measured by MTT assay. **(E).** The clone formation of HEK293 cells over a 10-day period after replating the cells transfected with the AK4 shRNA. The number of clones in the control shRNA was set as 100%. The average numbers and error bars were calculated from three independent experiments.

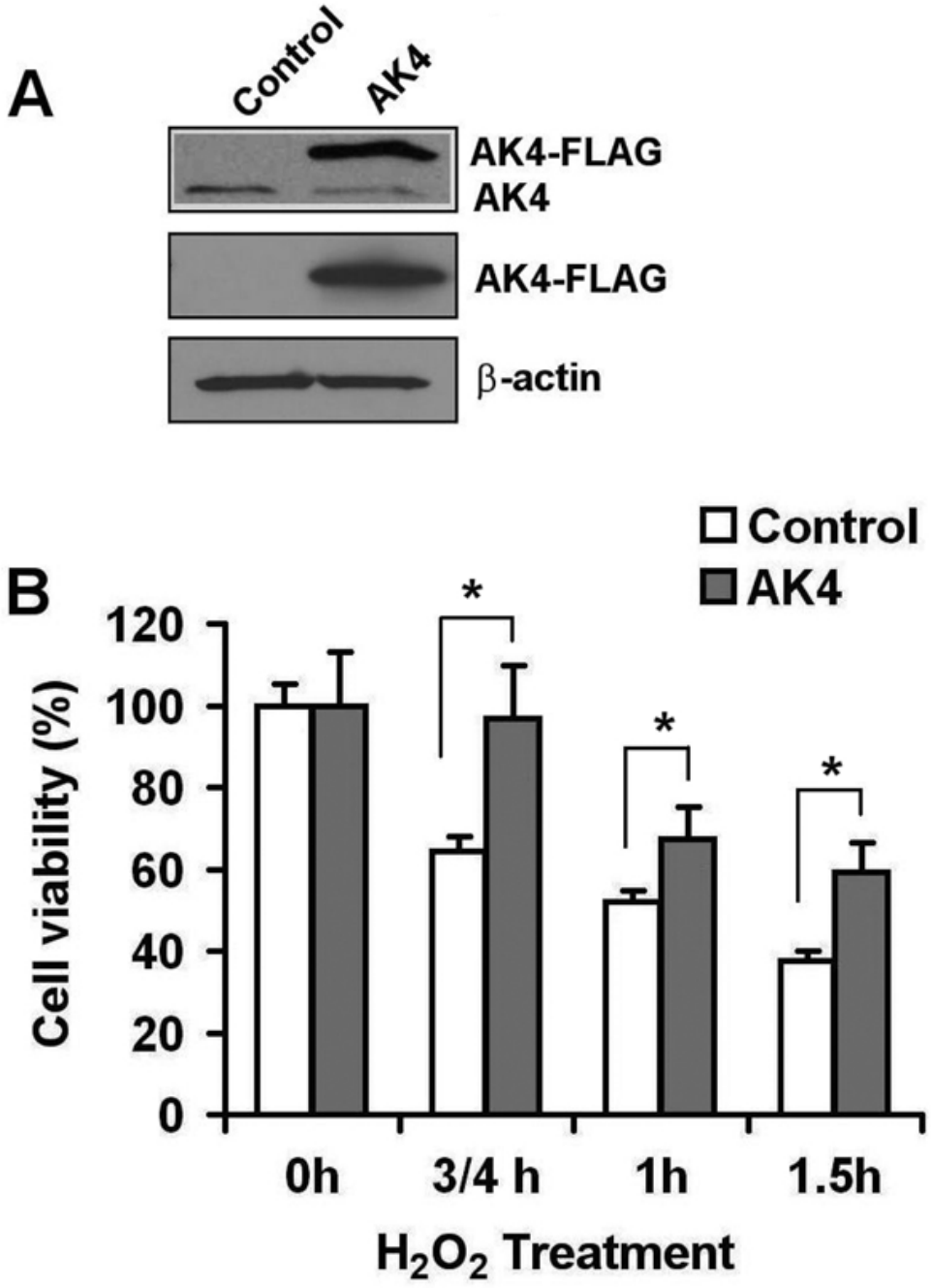

Figure 3. AK4 over-expression protected SH-SY5Y cells from H_2O_2 exposure

(A). AK4 over-expression was detected by Western blotting using AK4 (top) and FLAG (middle) antibodies, respectively. Western blotting of β-actin (bottom) was performed as a loading control.**(B).** The percentage of viable SH-SY5Y cells after H_2O_2 treatment for the indicated time period. The average values were calculated from three independent experiments. *: $p < 0.01$ using the Student's t-test.

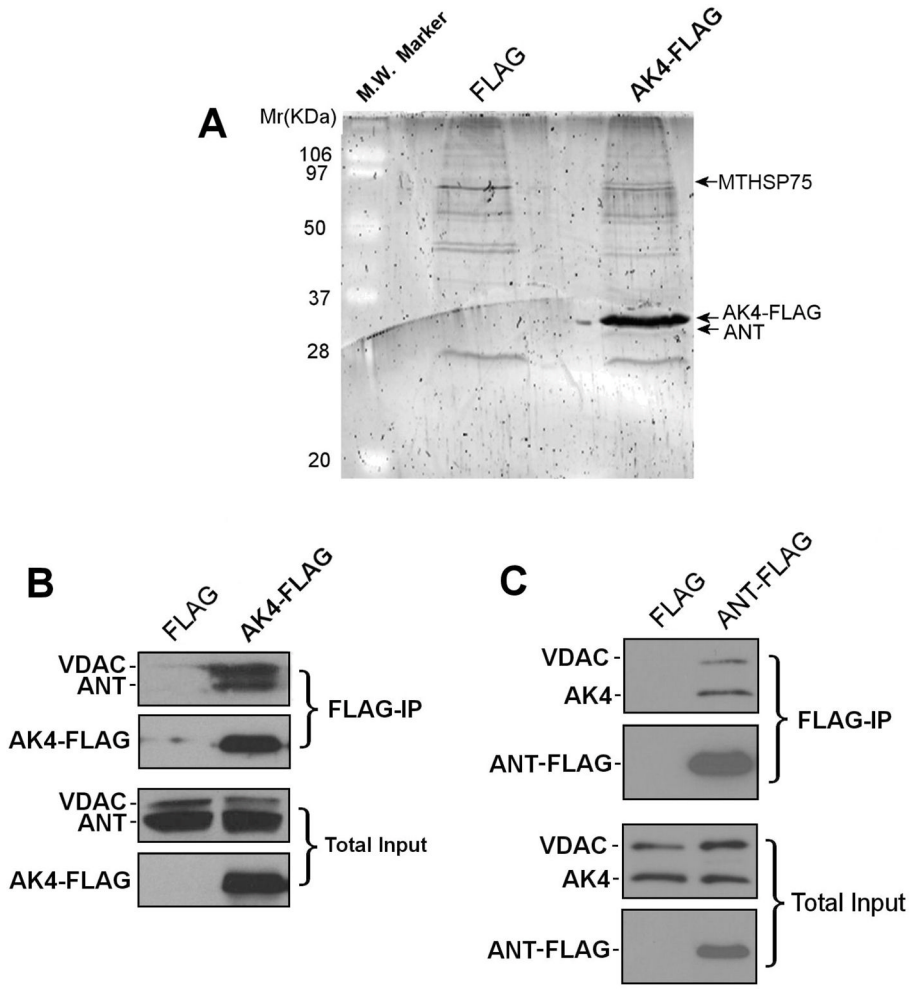

Figure 4. Interaction between AK4 and ANT

(A). The Sypro Ruby staining image of protein immunoprecipitated by AK4-FLAG from HEK293 cells over-expressing AK4-FLAG. Cells transfected with the FLAG vector were used as control in the IP experiments and three bands unique in the AK4-FLAG IP are indicated by arrow. Subsequent mass spectrometry identified the three proteins as indicated in the figure. **(B).** HEK293 were transfected with AK4-FLAG or FLAG control vector and cell lysate were subjected to AK4-FLAG IP. Both ANT and VDAC were co-precipitated with AK4-FLAG. Similar levels of endogenous ANT and VDAC were in both input samples. **(C).** HEK293 cells were transfected with ANT-FLAG or FLAG control vector and cell lysates were subjected to ANT-FLAG IP. Both AK4 and VDAC were co-precipitated with AK4-FLAG. Similar levels of endogenous AK4 and VDAC were in both input samples.

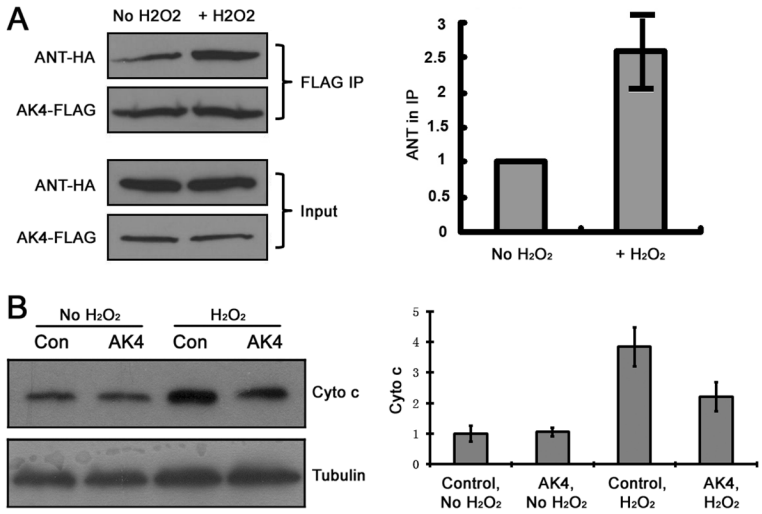

Figure 5. Increased amount of AK4-interacting ANT and suppressed cytochrome c release in AK4 over-expressing cells under oxidative stress

(A). Increased amount of ANT interacting with AK4 in cells exposed to H_2O_2. SH-SY5Y cells were transfected with AK4-FLAG and ANT-HA. Half of the cells were exposed to 150 μM H_2O_2 for 1 hour, cultured in normal medium for 3 additional hours before harvesting. The other half cells went through the same procedure but without H_2O_2. Cell lysates were subjected to AK4-FLAG IP and subsequent Western blotting analysis. Increased amount of ANT was co-precipitated with AK4 in the cells exposed to H_2O_2 treatment. Similar amount of AK4-FLAG and ANT-HA were expressed in the cells. Quantification of the amount of ANT co-precipitated with AK4 is shown in the bar graph. The Western band intensity of ANT was normalized with that of AK4 in the IP samples and the average values from three independent experiments are shown. **(B).** Suppressed cytochrome c release to cytosol in AK4 over-expressing cells exposed to 150 μM H_2O_2. SH-SY5Y cells were transfected with AK4-FLAG or FLAG control vector. Half of the cells were exposed to 150 μM H_2O_2 for 1 hour and the other half cells went through the same procedure but without H_2O_2. Cell lysates were subjected to sequential centrifugation to prepare the mitochondria-free cytosolic fraction. Western blotting was used to assess the amount of cytochrome c levels in the cytosolic fraction. Quantification of the amount of cytochrome c levels is shown in the bar graph. The Western band intensity of cytochrome c was normalized with that of tubulin and the average values from three independent experiments are shown.

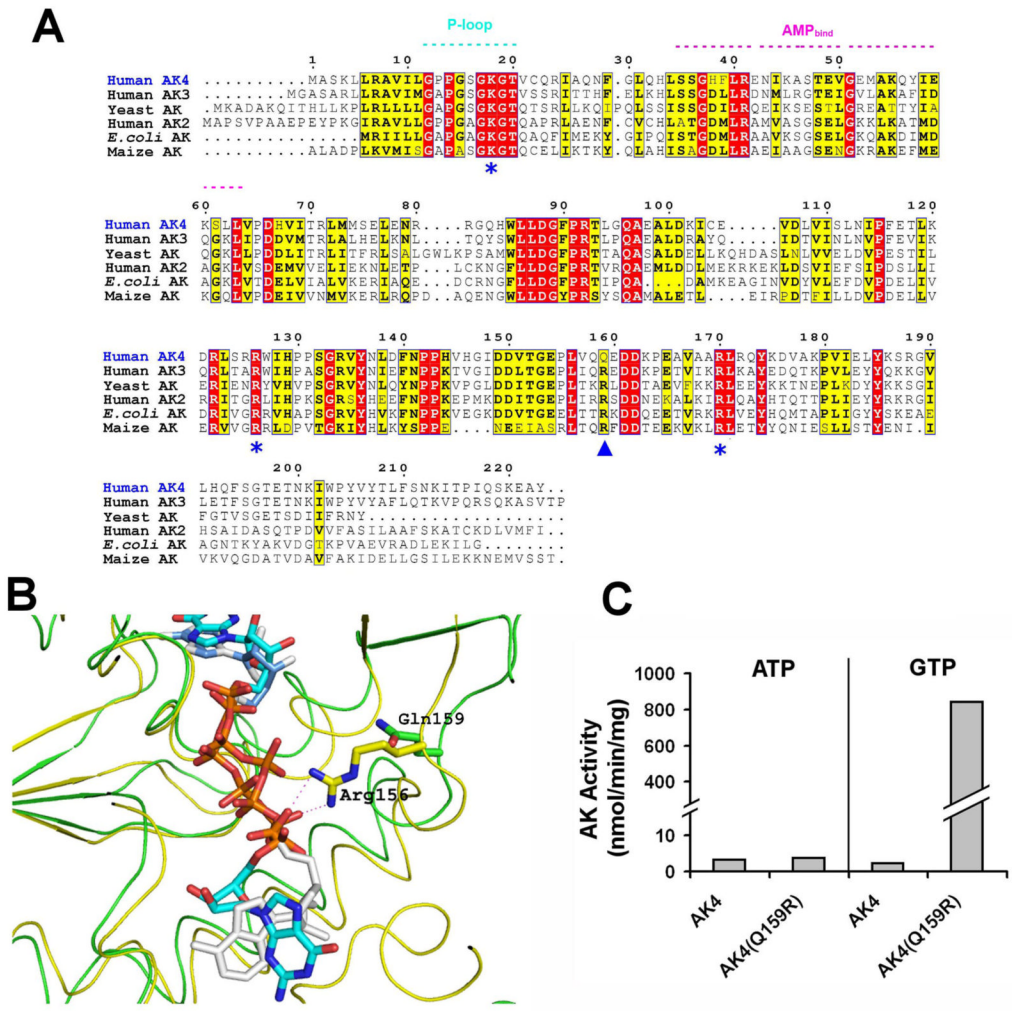

Figure 6. Analysis of AK4 structure and enzymatic inactivity

(A). Structure-based sequence alignment of human AK4 with human AK3, human AK2, *E.coli* AK, maize AK and yeast AK. Strictly conserved and conservatively substituted residues are boxed and marked with red and yellow background, respectively. The sequence numbers of human AK4 are shown in black above the sequence alignment. The AMP binding motif and the P-loop responsible for NTP binding are indicated. Lys13, Arg123 and Arg167 in *E.coli* AK (i.e. Lys18, Arg126 and Arg170 in human AK4) are marked with blue stars. Arg156 in *E.coli* AK (i.e. Gln159 in human AK4) is marked with blue triangle. The figure was generated using ESPript. **(B).** Structural superposition of GP5-bound human AK4 (PDB entry 2BBW, in green) and AP5A-bound *E. coli* AK (PDB entry 1AKE, in yellow). The ligands, Gln159 in human AK4 and Arg156 in *E. coli* AK are shown in sticks. **(C).** AK activity of wild-type and Q159R mutant human AK4. ATP and GTP were used in the activity assay as the phosphoryl group donor. The adenylate kinase activity with GTP as substrate was restored by the G159R mutation, supporting the critical role of the arginine residue in the active site.